A Method for Quick Assessment of CO_2 Storage Capacity in Closed and Semi-Closed Saline Formations

Quanlin Zhou*, Jens T. Birkholzer, Chin-Fu Tsang, and Jonny Rutqvist

Earth Sciences Division, Lawrence Berkeley National Laboratory,

University of California, Berkeley, CA 94720, USA

*Corresponding Author, Tel: 1-510-486-5748, Fax: 1-510-486-5686; Email: qzhou@lbl.gov, Mail Address: One Cyclotron Road, MS 90-1116

Abstract: Saline aquifers of high permeability bounded by overlying/underlying seals may be surrounded laterally by low-permeability zones, possibly caused by natural heterogeneity and/or faulting. Carbon dioxide (CO_2) injection into and storage in such "closed" systems with impervious seals, or "semi-closed" systems with nonideal (low-permeability) seals, is different from that in "open" systems, from which the displaced brine can easily escape laterally. In closed or semi-closed systems, the pressure buildup caused by continuous industrial-scale CO_2 injection may have a limiting effect on CO_2 storage capacity, because geomechanical damage caused by overpressure needs to be avoided. In this research, a simple analytical method was developed for the quick assessment of the CO_2 storage capacity in such closed and semi-closed systems. This quick-assessment method is based on the fact that native brine (of an equivalent volume) displaced by the cumulative injected CO_2 occupies additional pore volume within the storage formation and the seals, provided by pore and brine compressibility in response to pressure buildup. With nonideal seals, brine may also leak through the seals into overlying/underlying formations. The quick-assessment method calculates these brine displacement contributions in response to an estimated average pressure buildup in the storage reservoir. The CO_2 storage capacity and the transient domain-averaged pressure buildup estimated through the quick-assessment method were compared with the "true" values obtained using detailed numerical simulations of CO_2 and brine transport in a two-dimensional radial system. The good agreement indicates that the proposed method can produce reasonable approximations for storage-formation-seal systems of various geometric and hydrogeological properties.

Keywords: geological CO_2 sequestration; storage capacity; saline aquifer; pressure buildup; numerical simulation

1. Introduction

Geological carbon dioxide (CO_2) sequestration in deep formations (e.g., saline aquifers, gas and oil reservoirs, and coal beds) is a promising measure for mitigating the impact of climate change (Bachu et al., 1994, 2002; Koide et al., 1992; IPCC, 2005; van der Meer, 1992). Reliable estimates are needed for the CO_2 storage capacity of geologic basins (Bradshaw et al., 2007). Currently, basin-scale storage capacity is often estimated based on the effective pore volume of suitable formations (i.e., those formations with sufficient injectivity, size, and long-term CO_2 containment capability). The effectiveness, or the storage efficiency factor, of suitable formations describes the fraction of total pore space available for CO_2 storage, limited by heterogeneity, buoyancy effects, residual water saturation, etc. (Bachu and Adams, 2003). Guidelines for estimating the storage capacity of deep saline formations were recently developed by the Capacity and Fairways Subgroup of the Geological Working Group of the U.S. Department of Energy (USDOE) Carbon Sequestration Regional Partnerships (USDOE, 2007). The current practice generally involves estimating storage capacity of "open" formations (Figure 1, top), from which the native fluid can easily escape laterally and make room for the injected CO_2 (e.g., Doughty and Pruess, 2004; Holloway et al., 1996; Shafeen et al., 2004; van der Meer, 1995). For such open formations, the pressure buildup caused by CO_2 injection is usually not a limiting factor except for maximum bottom-hole pressure at the injection well. However, the large amount of native brine laterally displaced by injected CO_2 in open systems may have a hydrological and geochemical impact on shallow groundwater

resources (Birkholzer et al., 2007; Nicot, 2008), an issue not addressed directly in this paper.

In certain geological situations, a storage basin may be composed of a number of compartmentalized reservoirs laterally separated by low-permeability zones. These zones may be formed by natural heterogeneity and/or faulting. When such a reservoir, bounded vertically by impervious seals, is surrounded on all sides by barriers of very low permeability, this reservoir acts as a "closed" system (Figure 1, middle) (i.e., there is negligible hydraulic communication with other formations during the injection period of interest, usually 30–50 years). Evidence of such closed systems has been found in hydrocarbon reservoirs, as indicated by sharp changes in fluid pressure along their boundaries (Muggeridge et al., 2004; Neuzil, 1995; Puckette and Al-Shaieb, 2003). Examples of such closed systems also include natural CO_2 reservoirs of high purity, which can be used as analogues for geological CO_2 sequestration (e.g., Allis et al., 2001; Pearce et al., 1996; Stevens et al., 2001). When large volumes of CO_2 are injected into a compartmentalized formation, which acts like a closed system (with the time scale of interest being the CO_2 injection period), a significant pressure buildup will be produced (e.g., Holloway et al., 1996; Polak et al., 2004). This pressure buildup can severely limit the CO_2 storage capacity, because overpressure-associated geomechanical damage needs to be avoided (Rutqvist and Tsang, 2002; Rutqvist et al., 2007). In this case, the storage capacity mainly depends on pore and brine compressibilities that provide expanded pore space available for storing the injected CO_2, and on the maximum pressure buildup that the formation can sustain.

82 Of course, the overlying and underlying seals of a storage aquifer are not perfectly
83 impervious, allowing the pressure buildup caused by CO_2 injection and storage to
84 partially dissipate into and through these seals. In this case, the saline aquifer acts like a
85 "semi-closed" system (Figure 1, bottom), allowing some fraction of the displaced brine to
86 migrate into and through the overlying and underlying sealing units, which in turn would
87 increase the storage capacity for CO_2. (Meanwhile, the stored CO_2 is safely contained
88 within the storage formation because of permeability and capillary barriers.) The
89 importance of this vertical interlayer communication mostly depends on the permeability
90 of the seals, which can vary widely (from 10^{-23} to 10^{-16} m^2, or from 10^{-8} to 10^{-1} mD)
91 depending on their hydrogeological characteristics (e.g., Domenico and Schwartz, 1998;
92 Hart et al., 2006; Hovorka et al., 2001; Neuzil, 1994). Relatively permeable sealing units
93 (e.g., with permeability on the order of 10^{-18} m^2 or higher) may allow considerable
94 vertical brine leakage out of the storage reservoir over the injection period. In this case,
95 the pressure buildup may be reduced, and pressure constraints may not be a limiting
96 factor in CO_2 storage.

97 Our research aims at developing a method for the quick assessment of CO_2 storage
98 capacity in deep closed and semi-closed saline formations, complementing existing
99 methods for capacity estimates in open systems (USDOE, 2007). This method can be
100 used to estimate the storage efficiency factor and the transient domain-averaged pressure
101 buildup. The validity of the method is demonstrated by comparing the estimated storage
102 capacities to the "true" values calculated through detailed modeling of multiphase flow
103 and multicomponent transport of CO_2 and brine. The modeling was conducted using the
104 TOUGH2/ECO2N code, which has been tested and compared with other codes (Pruess,

105 2005; Pruess et al., 2004). The validity range is demonstrated for a range of hypothetical
106 formation-seal systems, with varying lateral radial extent (i.e., pore volume) and
107 hydrogeological properties (i.e., permeability and pore compressibility) of the storage
108 formation and sealing units.

109 **2. A Quick-Assessment Method for CO_2 Storage Capacity**

110 We developed a simple method for assessing the storage capacity of closed and semi-
111 closed storage formations. The basic principle is that CO_2 injection into these systems
112 will lead to pressurization (pressure buildup), because an additional volume of fluid
113 needs to be stored. The injected CO_2 displaces an equivalent volume of native brine,
114 which may either (1) be stored in the expanded pore space in the storage formation, (2)
115 be stored in the expanded pore space in the seals, or (3) leak through the seals into
116 overlying/underlying formations. The quick-assessment method predicts the pressure-
117 buildup history over a given injection period and the "actual" storage efficiency factor at
118 the end of injection. We define the storage efficiency factor, E, as the volumetric fraction
119 of stored CO_2, per unit initial total pore volume of the storage formation, similar to the
120 earlier definition for open systems (USDOE, 2007). The method is designed to provide
121 capacity estimates at early stages of site selection and characterization, when (1) quick
122 assessments of multiple sites may be needed and when (2) site characterization data are
123 rather sparse. More specifically, the estimated pressure increase caused by injection and
124 storage of a specified volume of CO_2 can be compared to a sustainable pressure
125 threshold, which is the maximum pressure that the formation can sustain without
126 geomechanical damage. Alternatively, one may determine the maximum CO_2 volume

that can be injected without jeopardizing the geomechanical structure of the formation-seal system.

2.1. Simplifications and Assumptions

Several simplifications and assumptions of both reservoir characteristics (geometric and hydrogeological properties) and processes made in the quick-assessment method are outlined below for an idealized, two-dimensional radial formation-seal system:

- The homogeneous storage formation for CO_2 sequestration is of radial extent R and thickness B_f, with an initial porosity ϕ_f. The initial total pore volume is $V_f = \phi_f A B_f = \pi R^2 \phi_f B_f$, where A is the horizontal area. The storage formation has a pore compressibility β_p $(= \frac{1}{\phi_f} \frac{\partial \phi'_f}{\partial p}$, where ϕ'_f is the storage formation porosity, dependent on pressure change), which includes the possible contribution of vertical formation expansion and reflects the confining pressure and overburden stress prior to CO_2 injection.
- The upper and lower homogeneous seals have a uniform, identical thickness, B_s, permeability k_s, porosity ϕ_s, and pore compressibility β_{ps}. The total pore volume of both seals is $V_s = 2\phi_s A B_s$.
- The native brine has compressibility, β_w $(= \frac{1}{\rho_w} \frac{\partial \rho_w}{\partial p})$, representing the change in brine density (ρ_w) in response to pressure buildup, and viscosity, μ_w, dependent on temperature, pressure, and salinity at the initial time of injection.
- The above hydrogeological parameters are assumed to be constant over the relevant range of pressure conditions, from the initial hydrostatic pressure to the elevated pressure value under final storage conditions. Only porosity changes are considered in response to pressure increases.
- The storage formation has uniform pressure buildup at any time of injection, independent of formation permeability. This overpressure decreases linearly through the seals to the hydrostatic pressure (prior to CO_2 injection) assumed at the top of the overlying seal and at the bottom of the underlying seal.

- All injected CO_2 mass is contained as a CO_2–rich phase, with negligible dissolved CO_2 mass within the storage formation. The total volume of stored CO_2 depends on CO_2 density, which in turn depends on temperature and transient pressure conditions.
- Native brine leakage occurs through the entire formation-seal interface with a uniform leakage rate, independent of CO_2 plume extent.

The validity of some of these assumptions is discussed in Section 4, based on the detailed simulation results presented in Section 3. Note that the storage formation can have any shape with varying thickness, because only its total pore volume is used in the quick-assessment method. Specifications on the geometry of the storage formation have been chosen for easier comparison with numerical simulation results.

2.2. Basic Equations

The quick-assessment method considers that the pore volume needed to store injected CO_2, $V_{CO2}(t_1)$, after a given injection time, t_1, is provided by three contributions: (1) the expanded storage volume in the storage formation resulting from pressure buildup, (2) the expanded storage volume within the seals resulting from pressure buildup, and (3) the volumetric leakage of brine into the formations above the upper seal and below the lower seal. The expanded storage volume is caused by both brine and pore compressibility. A simple expression describes this volumetric relationship, as follows:

$$V_{CO2}(t_1) = (\beta_p + \beta_w)\Delta p(t_1)V_f + 0.5(\beta_{ps} + \beta_w)\Delta p(t_1)V_s + \int_0^{t_1} \frac{2Ak_s\Delta p(t)}{\mu_w B_s} dt, \qquad (1)$$

where $\Delta p(t_1)$ is the pressure buildup at time t_1, $\Delta p(t)$ ($t = [0, t_1]$) is the transient pressure buildup from the beginning to the end of injection, and the factor of 0.5 stems from the assumption of linear pressure buildup from zero at the top of the overlying seal (and the bottom of the underlying seal) to the storage-formation value at the formation-

seal interfaces. Each of the three terms on the right-hand side of Equation (1) corresponds to one of the three storage contributions mentioned above. Equation (1) essentially links $V_{CO2}(t_1)$ to the average pressure buildup in the storage formation. By solving Equation (1) for t_1, the total pressure buildup in the closed or semi-closed formation can be assessed as a function of $V_{CO2}(t_1)$.

Based on the definition of the storage efficiency factor and Equation (1), the storage efficiency factor, $E(t_1)$, for a semi-closed system can be calculated:

$$E(t_1) = \left(\beta_p + \beta_w\right)\Delta p(t_1) + 0.5\left(\beta_{ps} + \beta_w\right)\frac{V_s}{V_f}\Delta p(t_1) + \int_0^{t_1}\frac{2Ak_s\Delta p(t)}{\mu_w B_s V_f}dt\,, \tag{2}$$

where the storage efficiency factor consists of three individual efficiency contributions from expanded pore volume in the storage formation and the seals, as well as from brine leakage into the underlying and overlying formations. To compare the relative importance of the three individual contributions, we define the volumetric fractions of displaced brine stored in the storage formation (F_f), in the seals (F_s), and in the overlying/underlying formations (F_l), relative to the total pore volume storing CO_2, as follows:

$$F_f = \left(\beta_p + \beta_w\right)\Delta p(t_1)V_f / V_{CO2}(t_1)\,, \tag{3a}$$

$$F_s = 0.5\left(\beta_{ps} + \beta_w\right)\Delta p(t_1)V_s / V_{CO2}(t_1)\,, \tag{3b}$$

$$F_l = \int_0^{t_1}\frac{2Ak_s\Delta p(t)}{\mu_w B_s}dt \Big/ V_{CO2}(t_1)\,. \tag{3c}$$

By definition, F_f, F_s, and F_l add up to one. Note that from these volumetric fractions, one can calculate the total volumes of the displaced brine leaking into other formations and stored in the seals and the storage formation, by multiplying these fractions by the volume of stored CO_2 at the final storage condition.

Note that V_{CO2} is not the total volume of CO_2 at the injection condition; it is the total pore volume occupied by injected CO_2 under the final storage condition, depending on the density of CO_2-rich phase. The necessary CO_2 storage capacity for a given site is often provided in total CO_2 mass, M_{CO2}, instead of V_{CO2}. Conversion of volume to mass is achieved through $M_{CO2} = \rho_{CO2}(t_1)V_{CO2}$, in which the CO_2 density, ρ_{CO2}, is evaluated at pressures and temperatures representing the final storage conditions. Because the pressure buildup caused by injection is not known beforehand for a given total CO_2 mass, the CO_2 density at storage conditions is either estimated a priori (in anticipation of an estimated pressure buildup) or determined in an iterative procedure, using the calculated average pressure to correct the density and vice versa.

2.3. Application to Closed Systems

In a closed system, the available volume for storage of CO_2 is provided only by the expansion of the pore volume and the increased brine density in response to pressure buildup in the storage formation. Equation (1) can then be simplified to the following linear expression:

$$V_{CO2}(t_1) = (\beta_p + \beta_w)\Delta p(t_1)V_f \quad . \tag{4}$$

This equation can be used, for example, to estimate the maximum storage capacity for a given sustainable pressure buildup, $\Delta p_{\max}$. Similarly, one can calculate the expected

average pressure buildup, $\Delta p(t_1)$, for a given total volume of stored CO_2 or a given CO_2 mass.

The storage efficiency factor of CO_2 storage in a closed system with average pressure buildup $\Delta p(t_1)$ can be derived from a simplification of Equation (2)

$$E = E_p\left(\Delta p(t_1)\right) + E_b\left(\Delta p(t_1)\right) = \left(\beta_p + \beta_w\right)\Delta p(t_1), \quad (5)$$

where E_p is the storage efficiency factor caused by pore compressibility, and E_b is the storage efficiency factor produced from brine compressibility. Inserting the sustainable pressure buildup, $\Delta p_{\max}$, into Equation (5) results in the maximum storage efficiency. For example, using $\Delta p_{\max} = 6.0$ MPa, a pore compressibility of 4.5×10^{-10} Pa^{-1} and a brine compressibility of 3.5×10^{-10} Pa^{-1}, we arrive at $E_p = 0.0027$ and $E_b = 0.0021$, and $E = 0.0048$. In other words, less than half a percent of the total pore volume of a closed system would be available for the volumetric storage of CO_2 in a closed system during the injection period.

2.4. Application to Semi-Closed Systems

Unlike the linear relationship of the total volumetric storage capacity and pressure buildup to pore and brine compressibilities for a closed system, such relationships for a semi-closed system are nonlinear and transient, with the pressure buildup in the storage formation affecting leakage rate through the seals, and vice versa. This makes solving of Equation (1) more complicated; however, a solution can be achieved through a simple numerical integration in time. For this purpose, the injection time period $[0, t_1]$ can be discretized into a number (n) of equally spaced time intervals of duration Δt to form a

time series: $t_{0,}\ t_1,...,\ t_{i-1},\ t_i,....,\ t_{n-1},\ t_n$, with $t_0 = 0$ and $t_n = t_I$. Equation (1) converts into its discrete form as follows:

$$\Delta p(t_i) = \frac{V_{CO2}(t_i) - \dfrac{2Ak_s\Delta t}{\mu_w B_s}\sum_{j=0}^{i-1}\Delta p(t_j)}{\left(\beta_p + \beta_w\right)V_f + 0.5\left(\beta_{ps} + \beta_w\right)V_s + \dfrac{Ak_s\Delta t}{\mu_w B_s}}\ ,\ i = [1,\ n]\,. \tag{6}$$

At each new time step, the pressure-buildup values at all previous time steps are known, such that the summation term in Equation (6) (representing the cumulative brine leakage from beginning of injection to the previous time step) can be executed. Equation (6) eventually yields the pressure buildup at all time steps from the beginning to the end of injection. Once Equation (6) has been solved, the storage efficiency factors in Equation (2) or the volumetric fractions in Equation (3) can be derived using the known injection and pressure history.

In the quick-assessment method, it is assumed that the semi-closed systems have a radial impervious layer to bound the systems laterally. This method may not be applicable to the systems bounded laterally by a permeable layer with a permeability value between those of the storage formation and the overlying/underlying sealing units.

Note that continued CO_2 injection into a semi-closed system would eventually lead to a steady-state condition at which the volumetric injection rate, Q_{CO2} (as a function of the steady-state storage condition), equals the rate of displaced brine leakage through the seals, assuming that the geomechanical and hydraulic integrity of the storage unit and seals is maintained. The pressure buildup, Δp_S, associated with this steady-state condition can be calculated as follows:

$$\Delta p_S = \frac{Q_{CO2}}{2Ak_s / \mu_w B_s}, \quad Q_{CO2} = \frac{G_{CO2}}{\rho_{CO2}(\Delta p_S)}, \tag{7}$$

where G_{CO2} is the injection rate of CO_2 mass. If Δp_S is unrealistically high, i.e., higher than the sustainable pressure buildup, the storage capacity is pressure constrained and needs to be evaluated, using Equation (6). If, on the other hand, Δp_S is relatively small, brine leakage through the seals is sufficient to allow for significant CO_2 storage without pressurization concerns. In this case, the semi-closed system acts like an open storage formation, and its storage capacity is not pressure-constrained.

2.5. Sustainable Pressure Buildup

The CO_2 storage capacity of pressure-constrained systems depends on the *sustainable pressure buildup* that a given formation-seal system is expected to tolerate without geomechanical degradation (such as microfracturing and/or fault reactivation) of the sealing structures (USEPA, 1994; Neuzil, 2003; Rutqvist and Tsang, 2002; Rutqvist et al., 2007). Fluid pressure in the storage formation may also be constrained to limit the pressure driving forces into neighboring formations, or to account for potential concerns about seismicity. According to Rutqvist et al. (2007), the sustainable pressure buildup should be reviewed on a case-by-case basis, taking into account initial stress fields and geomechanical properties of the rock units at the selected sites.

Some guidance on the determination of a sustainable pressure buildup (for geomechanical damage) is provided by the current practice for underground injection control of liquid wastes. The regulatory standard states that maximum injection pressure should be less than the measured *fracture closure pressure*. Below the fracture closure pressure, any existing fractures cannot open and no new fractures can form, implying no

280 enhanced migration of waste fluids out of the injection intervals (USEPA, 1994). The
281 regional guidance for implementation is that the maximum injection pressures can be
282 determined either by a site-specific fracture closure pressure derived from direct or
283 indirect testing, or by formation-specific default values for the fracture-closure pressure
284 gradients. For example, a default value of 0.0129 MPa/m (130% of the hydrostatic
285 pressure gradient) is given for the Mt. Simon Formation in Illinois, USA; 0.0181 MPa/m
286 (181% of the hydrostatic pressure gradient) is reported for the Dundee Limestone in the
287 Michigan Basin in USA. These fracture-closure pressure gradients correspond to
288 sustainable fluid pressures of 15.5 and 21.7 MPa at 1,200 m depth, leading to sustainable
289 pressure buildup of 3.5 and 9.7 MPa, respectively. In the following example applications,
290 we chose a sustainable pressure buildup of 6.0 MPa, which corresponds to 50% of the
291 initial hydrostatic pressure at the top (1,200 m) of the hypothetical storage formation.
292 This value was used to demonstrate the quick-assessment method, and a site-specific
293 value is needed when applied to a specific geologic site.

294 **3. Numerical Simulations and Results**

295 To validate the quick-assessment method discussed above, the "true" CO_2 storage
296 capacity of closed or semi-closed formations was calculated through numerical
297 simulation of the multiphase flow and multicomponent transport of CO_2 and brine in a
298 hypothetical deep saline formation, using the TOUGH2/ECO2N simulator (Pruess, 2005;
299 Pruess et al., 1999). The validity range of the quick-assessment method was demonstrated
300 using different simulation runs, varying the radial extent to evaluate the effect of storage
301 formation size, varying storage-formation properties to evaluate the uniformity of
302 pressure buildup, and varying seal permeability to investigate the effect of brine leakage

303 into and through the seals and its impact on storage capacity. For each simulation run, we
304 calculated the storage efficiency factor (E) and the domain-averaged pressure buildup. If
305 the simulated pressure buildup in the storage formation at the end of the injection period
306 is less than the sustainable pressure buildup, the designated storage scenario is not
307 pressure-constrained, and we refer to E as the *actual storage efficiency factor*. In contrast,
308 in cases where the simulated pressure buildup exceeds the sustainable pressure buildup
309 (which may occur before reaching the designated injection volume), the storage scenario
310 is pressure-constrained. In such cases, we refer to E as the *maximum storage efficiency*
311 *factor*, which corresponds to the sustainable pressure buildup.

312 **3.1. Model Setup**

313 A two-dimensional radially symmetric model domain was chosen to represent a deep
314 saline aquifer. The storage formation, located at a depth of approximately 1,200 m below
315 the ground surface, is 250 m thick and bounded at the top and bottom by sealing units
316 (caprock and baserock) of 60 m thick each. The outer lateral boundary has a no-flow
317 condition. In the base case, the model domain has a radial extent of 20 km, and the
318 sealing units are assumed to be impervious. Carbon dioxide is injected in a zone of 125 m
319 in thickness and 50 m in radial extent. Injection operates over 30 years at a rate of 120
320 kg/s (i.e., annual rate of 3.8 million tonnes of CO_2). The aquifer is initially fully brine-
321 saturated, assuming a hydrostatic fluid pressure distribution. Isothermal conditions are
322 modeled with a uniform temperature of 45ºC. Table 1 lists the assigned values of
323 hydrogeological properties typical of a homogeneous brine aquifer suitable for CO_2
324 storage. Note that the brine compressibility is intrinsically taken into account in
325 TOUGH2/ECO2N in terms of density variation with fluid pressure.

326 The capacity of CO_2 storage in a closed or semi-closed system depends on the
327 hydrogeological properties of the storage formation and the confining units (e.g.,
328 permeability, porosity, and pore compressibility), and the total pore volume of the storage
329 formation (e.g., thickness and radial extent). The sensitivity simulations conducted in this
330 study are listed in Table 2. In each sensitivity case, only the property of interest was
331 changed from the base-case value. The van Genuchten model was used to calculate the
332 capillary pressure and the relative permeabilities for the two phase flow in all the
333 simulation cases (van Genuchten, 1980). This model contains two fitting parameters α
334 and m; the van Genuchten α parameter represents the inverse of the characteristic
335 capillary pressure or roughly of the entry pressure for the nonwetting phase and the van
336 Genuchten m parameter is a measure of the pore-size distribution. The α and m values of
337 the storage formation used in the simulations are 5.1×10^{-5} Pa^{-1} and 0.46, respectively
338 (Table 1). In Cases 10 through 13 with imperfect seals, the seal porosity and α
339 parameter are 0.05 and 5.1×10^{-6} Pa^{-1}, respectively. All other properties of the seals are
340 identical to the storage formation. In the model, fixed hydrostatic pressure conditions are
341 set at the top of the upper seal and the bottom of the lower seal.

342 **3.2. Results and Discussion**

343 Figures 2a and 2b show the spatial distributions of CO_2 saturation and pressure buildup
344 (compared to the initial hydrostatic pressure) at the end of the 30-year injection period for
345 the base case. The CO_2 plume is approximately 4 km wide and is concentrated at the top
346 portion of the aquifer, a result of the buoyant CO_2 accumulating below the impervious
347 caprock. As shown in Figure 2b, the region of elevated pressure is much larger than the
348 CO_2 plume size. In fact, a substantial pressure increase is observed throughout the entire

20 km model domain, with the pressure buildup at the outer radial boundary at approximately 4.5 MPa. The pressure buildup near the injection zone is slightly higher than 6.0 MPa, thus exceeding the assumed sustainable threshold. Notice that the pressure-buildup contour lines away from the CO_2 plume region are mostly vertical, indicating horizontal brine displacement. Nonvertical contour lines can be seen in the CO_2 plume region, where the pressure conditions are affected by buoyancy and nonlinearity inherent in two-phase flow processes. We may conclude that this example features a pressure-constrained formation near or slightly beyond its capacity limits at the end of the designated injection time.

Radial pressure-buildup profiles at different times throughout the injection period are shown in Figure 3. At the very beginning of injection, the injected CO_2 displaces native brine in the area very close to the injection zone. The strong initial pressure buildup results from (1) the driving forces needed to move native brine away from the injection zone and (2) phase interference between aqueous and CO_2 phases in the region of two-phase flow (Pruess and Garcia, 2002). This pressure increase, referred to here as *injection-driven pressure buildup*, depends on the boundary condition (i.e., CO_2 injection rate in the injection zone, injection strategy), formation permeability, and two-phase flow conditions. The pressure pulse propagates away from the injection zone and reaches the outer radial boundary after approximately two years. After that, the pressure at the outer boundary starts to increase with injection time in an approximately linear manner; i.e., the entire model domain becomes overpressurized such that additional pore volume is made available to store the injected CO_2. The pressure buildup related to the need for generating additional pore space is referred to as *storage-driven pressure buildup*, which

372 depends mainly on the pore compressibility of the formation (as well as on changes in
373 brine density).

374 Cases 1 through 5 analyze different storage formation sizes, with radial extent ranging
375 from 10 km to 100 km, including scenarios that range from clearly pressure-constrained
376 to not pressure-constrained for the given injection volume. Figures 2c and 2d show the
377 spatial distribution of CO_2 saturation and pressure buildup at the end of the 30-year
378 injection period for the case of a domain of 100 km radial extent. Comparison of Figures
379 2a and 2c indicates that the CO_2 plumes in both cases are generally similar in shape, with
380 minor differences in the lateral extent of the plumes caused by differences in pressure
381 buildup and thus CO_2 density. In contrast to the small difference in CO_2 plume extent, a
382 significant difference in the pressure conditions is observed in Figures 2b and 2d. The
383 larger model domain is not pressure-constrained, representing the pressure conditions of
384 an open system. As a result, the maximum pressure increase near the injection zone,
385 about half of which is observed in the 20 km case, mainly represents injection-driven
386 pressure buildup. At a radial distance of 20 km, the pressure buildup is 0.8 MPa in the
387 100 km case, significantly lower than the 4.5 MPa observed in the 20 km case. In the 10
388 km case (not shown), the simulated total pressure buildup actually reaches an
389 unrealistically high level at the end of 30-year injection, with maximum values above
390 18.0 MPa. Injection would have to cease after approximately eight years to keep the
391 actual pressure buildup smaller than the sustainable threshold of 6.0 MPa.

392 Figure 4 shows the sensitivity of local pressure buildup near the injection zone to the
393 permeability and pore compressibility of the storage formation. For the case with higher
394 permeability (one order of magnitude higher than the base case), the pressure buildup in

the formation is almost uniform over the entire domain, varying from 5.1 MPa close to the injection zone to 4.7 MPa at the outer boundary (Figure 4a). For the second case with a lower permeability (a factor of two lower than the base case), a strong local pressure buildup near the injection zone leads to fluid pressure buildup in excess of the assumed sustainable threshold of 6.0 MPa—see Figure 4b. As a result, the permeability of the storage formation influences both the uniformity of pressure buildup over the domain and the propagation velocity of the pressure pulse away from injection zone. This behavior can be explained easily using the two-dimensional radial flow equation (i.e., the diffusion equation for pressure propagation), and the diffusivity defined by $D_d = k/[\phi_f(\beta_w + \beta_p)\mu_w]$, neglecting the two-phase flow within the CO_2 plume (de Marsily, 1986; Muggeridge et al., 2004). Pressure dissipates (diffuses) faster for higher permeability and/or lower compressibility.

As shown in Figures 4c and 4d, the domain-averaged pressure buildup at 30 years is 0.8 and 9.0 MPa for the pore compressibility of 4.5×10^{-9} and 4.5×10^{-11} Pa^{-1}, respectively. This indicates that for the case of lower pore compressibility, the system will be pressure-constrained, and the designated CO_2 mass cannot be safely injected into the closed system without geomechanical damage. The pore compressibility of the storage formation is a key input parameter in the quick-assessment method. Wide ranges of pore compressibility have been reported in the literature, depending on the subsurface materials (e.g., Fjaer et al., 1991; Domenico and Schwartz, 1998; Hart, 2000; Harris, 2006).

Figure 5 shows horizontal profiles of pressure buildup at the top of the storage formation, as a function of seal permeability. The pressure buildup observed in the storage formation is very sensitive to increases in seal permeability. While the lowest seal permeability (10^{-20} m^2 or 10^{-5} mD) shows a behavior similar to the closed system for the time scale relevant to estimating CO_2 storage capacity (i.e., the injection time period), we see a strong reduction of overall pressure buildup in all other cases, particularly those with permeabilities of 10^{-18} and 10^{-17} m^2. In these cases, a significant fraction (e.g., 0.46 and 0.93) of the displaced brine escapes from the storage formation into the seals, and through the seals into the overlying and underlying formations during the injection period of 30 years, thereby providing additional storage capacity for the injected CO_2 such that less pressure buildup occurs. We have calculated the cumulative fraction of displaced brine escaping from the storage formation relative to the total volume of stored CO_2 at in-situ conditions. With a seal permeability of 10^{-20} m^2 (10^{-5} mD), this volume fraction is rather insignificant at 0.07, whereas with a seal permeability of 10^{-17} m^2 (10^{-2} mD), this fraction increases to 0.93; i.e., the additional CO_2 storage capacity from brine leakage would amount to about 93% of the total injected CO_2 at 30 years. (In the latter case, the average Darcy's velocity in the seals is approximately 2.0 mm/year for the steady-state condition.) This effect can be very important for storage-capacity estimates in compartmentalized systems that have sealing units with small, but non-zero, permeability. Notice that the pressure profiles in Figure 5d remain relatively unchanged after a few years of injection, indicating that a quasi-steady state has been reached in which the volumetric rate of leakage of displaced brine is identical to the volumetric rate of injected CO_2 under final storage conditions.

In contrast to the significant leakage of displaced brine, negligible amounts of CO_2 escape from the storage formation into the seals. The cumulative fractions of CO_2 leaking into the caprock are 0.22, 0.35, 0.70, and 3.1% of the total injected CO_2 mass, for the seal permeability cases of 10^{-20} (10^{-5} mD) to 10^{-17} m^2 (10^{-2} mD) respectively. Most of this leakage is dissolved CO_2 that the quick-assessment method cannot account for, migrating with leaking brine from the storage formation into the seals. Carbon dioxide as the nonwetting-phase fluid needs to overcome a considerable capillary entry pressure before being able to migrate into the water-saturated pores of the sealing units. The observed migration of CO_2 within the seals is limited to the immediate vicinity of the storage formation; CO_2 is not able to escape into units overlying or underlying the seals. When a higher entry pressure is used (as represented by a smaller site-specific value of the van Genuchten α parameter), the CO_2 phase leakage will be smaller.

The simulation results suggest that compartmentalized storage reservoirs with reasonably good, but imperfect, seals may allow for enough displaced brine leaking out of the formation to offset pressure-related storage limitations, while still having sufficient sealing capacity to trap supercritical CO_2. Seal permeabilities can range over orders of magnitude, from 10^{-23} to 10^{-16} m^2 (Domenico and Schwartz, 1998; Hart et al., 2006; Hovorka et al., 2001; Neuzil, 1994). Relevant to geological CO_2 sequestration, the measured permeability of the sealing unit overlying the storage formation is 1.0×10^{-18} m^2 (10^{-3} mD) at the Frio test site (Doughty and Pruess, 2004; Hovorka et al., 2001), and 0.75 to 1.5×10^{-18} m^2 at the Sleipner site (Chadwick et al., 2007).

4. Validity of the Quick-Assessment Method

To validate the quick-assessment method, we derived quick estimates of domain-averaged pressure buildup and storage efficiency factors for the simulation scenarios discussed above, and compared those estimates with their corresponding "true" values obtained via detailed numerical simulations.

4.1. Comparison of Pressure-Buildup Estimates

The first step in demonstrating the validity of the quick-assessment method is to compare the estimated domain-averaged pressure buildup against the numerical simulation results for both closed and semi-closed systems. Figure 6a shows domain-averaged pressure buildup, as a function of injection time, for closed systems of varying total pore volume (Cases 1 through 5 in Table 2). The quick-assessment estimates have been obtained using Equation (4), solving for pressure buildup $\Delta p(t)$ at given times t during the injection period. The corresponding cumulative CO_2 volume $V_{CO2}(t)$ at each time step t is derived from the constant CO_2 injection rate of 120 kg/s used in the numerical simulation, and the CO_2 density under the storage condition. Conversion from CO_2 mass to CO_2 volume is conducted at each time step using the CO_2 density calculated at average pressure conditions. The agreement between the true numerical solutions and the quick estimates is excellent, considering that several simplifications and assumptions are involved in the quick-assessment method (e.g., uniform pressure buildup in domain, no dissolution, constant compressibility values). In Case 2, with 10 km radial extent, pressure builds up to values exceeding the sustainable pressure threshold soon after injection.

Figures 6b and 6c show domain-averaged pressure buildup for the closed-system cases with varying formation permeability (Cases 1, 6, and 7 in Table 2) and varying pore

compressibility (Cases 1, 8, and 9 in Table 2), for a radial extent of 20 km. The results of the quick-assessment method are independent of formation permeability, and only one profile obtained by the quick-assessment method is shown in Figure 6b. The agreement between simulated and estimated average pressure buildup is very good. While formation permeability defines the magnitude of local injection-driven pressure buildup (see Figure 4), the average pressure change over the entire domain is hardly affected by permeability changes. Pore compressibility, in contrast, has a strong impact on the average pressure buildup in response to CO_2 injection (Figure 6c). In the case with the lowest pore compressibility, pressure buildup is so strong that the designated CO_2 volume cannot be safely stored. Since pore compressibility is a parameter explicitly accounted for in the quick-assessment method, the quick-assessment estimates provide an accurate representation of the detailed simulation results.

Figure 6d shows a similar comparison of domain-averaged pressure buildup for the semi-closed system with nonideal seals of different permeability (Cases 10 through 13). In these cases, the quick-assessment estimates are obtained using Equation (6). Overall, the agreement between estimated and numerical results is reasonably good, with a maximum discrepancy of less than 6%. While the quick-assessment method captures well the general transient, nonlinear trends in pressure buildup, it slightly underestimates the pressure buildup for the case with the lowest seal permeability (i.e., 10^{-20} m^2 or 10^{-5} mD) and slightly overestimates pressure buildup in the cases with relatively high seal permeability (e.g., 10^{-17} m^2 or 10^{-2} mD).

Both numerical and estimated results show clearly that the average pressure approaches an asymptotic maximum after a few years for the case with the relatively high seal permeability of 10^{-17} m^2 (Figure 6d). This indicates a steady-state condition with equal volumetric rates of CO_2 entering and displaced brine leaving the storage formation. We

apply Equation (7) to estimate the average pressure buildup that would correspond to such a condition and arrive at values of 0.34, 3.23, and 27.02 MPa for the three cases with seal permeabilities of 10^{-17}, 10^{-18}, and 10^{-19} m^2 (10^{-2}, 10^{-3}, 10^{-4} mD), respectively. In the first case, the estimated value is identical to the final pressure buildup shown in Figure 6d. In the second case, a steady-state condition has not yet been established after 30 years of injection, but would be reached if injection would continue for a few more years. The pressure value of 3.23 MPa associated with this steady-state condition is less than the sustainable pressure threshold, indicating that this scenario would not be pressure-constrained even if the injection period were much longer. In the third case, however, with a seal permeability of 10^{-19} (10^{-4} mD) or less, a steady-state condition cannot be reached without geomechanical degradation.

In summary, the quick-assessment method provides reliable pressure estimates that can be compared with the sustainable pressure buildup to judge whether the designated volume of CO_2 can be safely stored in a storage formation, with or without vertical interlayer communication with other formations.

4.2. Comparison of Storage Efficiency Factors for Closed Systems

We now compare the calculated and estimated (actual) storage efficiency factors of CO_2 storage in a closed system with different total pore volume (i.e., radial extents of 10, 20, 30, 50, 100 km). The estimated values are obtained using Equation (5) and the pressure buildup calculated from Equation (4) for the same injection and storage-formation conditions as in the numerical simulations. We calculate the actual storage efficiency factor corresponding to the considered scenarios of injection and observed pressure buildup, regardless of whether this pressure buildup is higher than the sustainable

pressure buildup. Notice that the simulated storage efficiency factors include storage contributions from CO_2 in supercritical phase, as well as CO_2 dissolved in brine.

Table 3 shows the comparison of the actual storage efficiency factors for each case after 30 years of injection, indicating reasonable agreement between estimated and calculated results. The quick-assessment estimates are slightly higher than those obtained through detailed numerical simulations. The significant decrease in the actual storage efficiency factor is observed with the increase in the radial extent, because of the decrease in the pressure buildup. In comparison, the maximum storage efficiency factor, calculated using the sustainable pressure buildup of 6.0 MPa and assigned brine and pore compressibilities would be $E = 0.0048$. The calculated actual storage efficiency factors can be evaluated against the maximum storage efficiency factor to check whether the designated CO_2 volume can be safely stored.

4.3. Comparison of Storage Contributions for Semi-Closed Systems

In this validation exercise, we compare the three volumetric fractions for a semi-closed system obtained through the quick-assessment method (using Equations 3a through 3c) against those directly derived from the numerical simulations. Table 4 summarizes the results at the end of the 30-year injection period for the different seal permeability cases. Most of the storage capacity is provided by the storage formation when seal permeability is low (e.g., more than 90% for seal permeability of 10^{-20} m^2 or 10^{-5} mD). In contrast, most of the storage capacity is provided by brine escaping through the seals when seal permeability is comparably high (e.g., more than 90% for seal permeability of 10^{-17} m^2 or 10^{-2} mD). In all cases, the match between the simulated and estimated fractions is reasonably good. The largest relative discrepancies occur with respect to the seal storage

554 of brine, because of the assumed linear pressure variation within the seals in the quick-
555 assessment method.

556 **4.4. Adequacy of Important Assumptions and Simplifications**

557 As shown in the above comparisons, the quick-assessment method provides reasonable
558 estimates for the CO_2 storage capacity and pressure buildup in closed and semi-closed
559 saline formations at various conditions. The accuracy of these estimates depends on the
560 degree to which the process-related assumptions are satisfied in a real problem. One
561 assumption is that the pressure buildup throughout the entire storage formation is
562 uniform. This assumption works well as long as the average pressure is reasonably
563 representative of the true pressure conditions (or, in other words, if the injection-driven
564 pressure buildup is less important than the storage-driven pressure buildup). The detailed
565 simulations in Section 3.2 feature one sensitivity case with small formation permeability
566 of 5×10^{-14} m^2 (50 mD), where injection pressure alone exceeds the sustainable threshold.
567 The quick-assessment method is not applicable in this case.

568 We generally recommend judging the quick-assessment results with care, knowing that
569 average pressure predictions may underestimate the local conditions near the injection
570 zone. On the other hand, the assumption of negligible CO_2 dissolution leads to an
571 overestimation of pressure buildup and an underestimation of CO_2 storage capacity. The
572 resultant approximation error depends on the CO_2 solubility in brine (which in turn varies
573 with pressure, temperature, and salinity) and the fraction of CO_2 in contact with water.
574 The detailed numerical simulations presented in this study suggest that the mass fraction
575 of CO_2 dissolved in brine ranges from 0.02 to 0.03, and that the dissolved CO_2 accounts
576 for approximately 7% of the total injected CO_2 mass at the end of 30-year injection.

577 Carbon dioxide density is calculated based on the estimated domain-averaged pressure
578 buildup at storage conditions and the initial hydrostatic pressure. The density calculation
579 captures transient pressure changes, but still introduces some inaccuracies because the
580 domain-averaged pressure buildup may differ from actual pressure conditions within the
581 CO_2 plume (which, of course, define CO_2 density). For native brine, the assumption of
582 constant viscosity and compressibility leads to negligible errors over the pressure range
583 relevant in this study.

584 **5. Summary and Conclusions**

585 We evaluated the CO_2 storage capacity in compartmentalized structures, where potential
586 storage formations are bounded laterally and by overlying/underlying seals. If CO_2 is
587 injected at an industrial scale into such closed systems (with impervious seals) or semi-
588 closed systems (with non-ideal seals), pressure buildup can have a limiting effect on CO_2
589 storage capacity. We developed a simple quick-assessment method to assess the expected
590 pressure buildup and CO_2 storage capacity in such potentially pressure-constrained
591 systems. For validation of the method, we used "true" results from a numerical
592 simulation model, which captures all relevant multiphase processes, determining the
593 transient pressure buildup and CO_2 plume evolution in a hypothetical two-dimensional
594 radial system.

595 The validity of the proposed method was demonstrated by the good agreement between
596 the simple estimates and the numerical results regarding (1) the pressure buildup history
597 over the injection period and (2) the storage efficiency factor calculated at the end of the
598 injection period. We consider the new method useful for site selection and
599 characterization, when storage capacity estimates may have to be compared over a large

number of sites. For a storage formation of relatively low permeability, the quick-assessment method may not be suitable because of low injectivity and high degree of non-uniformity of the pressure field, and detailed numerical simulations are required.

One interesting finding of this research is the importance of upper- and lower-seal permeability on pressure buildup in the storage formation. Closed systems with impermeable seals allow CO_2 storage only up to the point at which pressure in the storage formation approaches a sustainable threshold. This pressure constraint translates into small storage efficiency, on the order of 0.5% of the initial pore space for a typical pore compressibility value. However, only storage-formation-seal systems with very low seal permeabilities of 10^{-20} m^2 or less exhibit such a closed-system behavior at the time scale of interest to capacity estimation; i.e., the leakage of native brine into and through the bounding seals is so small that the observed pressure buildup is similar to a closed system. With seal permeability varying from 10^{-19} to 10^{-17} m^2, brine leakage into and through the seals had a moderate to strong effect in reducing or limiting the pressure buildup in the storage formation, thus allowing for considerably higher storage efficiency, while CO_2 was still safely trapped because of the combined capillary and permeability barriers. Our results indicate that a semi-closed system with seal permeability of 10^{-17} m^2 is essentially an open system with respect to pressure buildup, because the rate of displaced brine leaking through the seals equals the rate of injected CO_2 at a later time of injection.

Acknowledgments

The authors wish to thank Curtis M. Oldenburg at Lawrence Berkeley National Laboratory (LBNL) for his careful internal review of the manuscript. Thanks are also due

623 to Dr. Stefan Bachu, the Associate Editor, and two anonymous reviewers for their
624 constructive suggestions for improving the quality of the manuscript. This work was
625 funded by the Assistant Secretary for Fossil Energy, Office of Sequestration, Hydrogen,
626 and Clean Coal Fuels, National Energy Technology Laboratory, of the U.S. Department
627 of Energy, and by Lawrence Berkeley National Laboratory under Contract No. DE-
628 AC02-05CH11231.

629 **References**

630 Allis, R., Chidsey, T., Gwynn, W, Morgan, C., White, S., Adams, M., Moore, J., 2001.
631 Natural CO_2 reservoirs on the Colorado Plateau and Southern Rocky Mountains:
632 Candidates for CO_2 sequestration, in the Proceedings of First National Conference
633 of Carbon Sequestration, National Energy Technology Laboratory, Washington
634 DC, USA, May 15-17, 2001.

635 Bachu, S., 2002. Sequestration of CO_2 in geological media in response to climate change:
636 road map for site selection using the transform of the geological space into the CO_2
637 phase space. Energy Convers. Manage. 43, 87-102.

638 Bachu, S., Adams, J.J., 2003. Sequestration of CO_2 in geological media in response to
639 climate change: capacity of deep saline aquifers to sequester CO_2 in solution.
640 Energy Convers. Manage. 44, 3151–3175.

641 Bachu, S., Gunter, W.D., Perkins, E.H., 1994. Aquifer disposal of CO_2: Hydrodynamic
642 and mineral trapping. Energy Convers. Manage. 35(4), 269–279.

643 Birkholzer, J.T., Zhou, Q., Rutqvist, J., Jordan, P., Zhang, K., Tsang, C.-F., 2007.
644 Research Project on CO_2 Geological Storage and Groundwater Resources: Large-
645 Scale Hydrogeological Evaluation and Impact on Groundwater Systems, Report
646 LBNL-63544, Lawrence Berkeley National Laboratory, Berkeley, CA, USA.

647 Bradshaw, J., Bachu, S., Bonijoly, D., Burruss, R., Holloway, S., Christensen, N.P.,
648 Mathiassen, O.M., 2007. CO_2 storage capacity estimation: issues and development
649 of standards. International J. Greenhouse Gas Control 1(1), 62-68.

650 de Marsily, G., 1986. Quantitative Hydrogeology, Academic Press, Inc, San Diego.

651 Domenico, P.A., Schwartz, F.W., 1998. Physical and Chemical Hydrogeology, 2nd ed.
652 John Wiley & Sons, Inc., New York.

653 Doughty, C., Pruess, K., 2004. Modeling supercritical carbon dioxide injection in
654 heterogeneous porous media. Vadose Zone J. 3, 837–847.

655 Fjaer, E., Holt, R.M., Horsrud, P., Raaen, A.M., 1991. Petroleum Related Rock
656 Mechanics. Elsevier, Amsterdam.

657 Harris, J.M., 2006. Seismic Monitoring of CO_2 Sequestration, GCEP Technical Report,
658 Stanford University, Palo Alto, CA, USA.

659 Hart, D.J., 2000. Laboratory Measurements of Poroelastic Constants and Flow
660 Parameters and Some Associated Phenomena. Ph.D. Thesis, University of
661 Wisconsin-Madison, Madison, WI, USA.

662 Hart, D.J., Bradbury, K.R., Feinstein, D.T., 2006. The vertical hydraulic conductivity of
663 an aquitard at two spatial scales. Ground Water 44(2), 201-211.

664 Holloway, S., Heederik, J.P., van der Meer, L.G.H., Czemichowski-Lauriol, I., Harrison,
665 R., Lindeberg, E., Summerfield, I.R., Rochelle, C., Schwarzkopf, T., Kaarstad, O.,
666 Berger, B., 1996. The Underground Disposal of Carbon Dioxide: Summary Report,
667 JOULE II Project No. CT92-0031, British Geological Survey, Keyworth, UK.

668 Hovorka, S.D., Doughty, C., Knox, P.R., Green, C.T., Pruess, K., Benson, S.M., 2001.
669 Evaluation of brine-bearing sands of the Frio formation, upper Texas gulf coast for
670 geological sequestration of CO_2, in: First National Conference on Carbon
671 Sequestration, National Energy Technology Laboratory, Pittsburgh, PA, USA, 14–
672 17 May, 2001.

673 IPCC (Intergovernmental Panel on Climate Change), 2005. IPCC Special Report on
674 Carbon Dioxide Capture and Storage. Cambridge University Press, New York.

675 Koide, H., Tazaki, Y., Noguchi, Y., Nakayama, S., Iijima, M., Ito, K., Shindo, Y., 1992.
676 Subterranean containment and long-term storage of carbon dioxide in unused
677 aquifers and in depleted natural gas reservoirs. Energy Convers. Manage. 33(5–8),
678 619–626.

679 Muggeridge, A., Abacioglu, Y., England, W., Smalley, C., 2004. Dissipation of
680 anomalous pressures in the subsurface. J. Geophys. Res. 109, B11104,
681 doi:10.1029/2003JB002922.

682 Neuzil, C.E., 1994. How permeable are clays and shales? Water Resour. Res. 30(2), 145–
683 150.

684 Neuzil, C.E, 1995. Abnormal pressures as hydrodynamic phenomena. Am. J. Science
685 295, 742-786.

686 Neuzil, C.E., 2003. Hydromechanical coupling in geologic processes. Hydrogeol. J. 11,
687 41–83, DOI:10.1007/s10040-002-0230-8.

688 Nicot, J.-P., 2008. Evaluation of large-scale CO_2 storage on fresh-water sections of
689 aquifers: an example from the Texas Gulf Coast Basin. International J. Greenhouse
690 Gas Control (in revision).

691 Pearce, J.M., Holloway, S., Wacker, H., Nelis, M.K., Rochelle, C., Bateman, K., 1996.
692 Natural occurrence as analogues for the geological disposal of carbon dioxide.
693 Energy Convers. Manage. 37(6-8), 1123-1128.

694 Polak, S., Lundin, E., Bøe, R., Lindeberg, E.G.B., Olesen, O., Zweigel, P. 2004. Storage
695 Potential for CO_2 in the Beitstadfjord Basin, Mid-Norway, Report SINTEF No.
696 54.5272.00/01/04 and NGU No. 2004.036. 51p, Geological Survey of Norway,
697 Trondheim, Norway.

698 Pruess, K., 2005. ECO2N: A TOUGH2 Fluid Property Module for Mixtures of Water,
699 NaCl, and CO_2, Report LBNL-57952, Lawrence Berkeley National Laboratory,
700 Berkeley, CA, USA.

701 Pruess, K., Garcia, J., 2002. Multiphase flow dynamics during CO_2 disposal into saline
702 aquifers. Environ. Geol. 42, 282–295.

703 Pruess, K., Oldenburg, C.M., Moridis, G., 1999. TOUGH2 User's Guide, version 2.0.
704 Report LBNL-43134, Lawrence Berkeley National Laboratory, Berkeley, CA,
705 USA.

706 Pruess K., García, J., Kovscek, T., Oldenburg, C. M., Rutqvist, J., Steefel, C., and Xu, T.,
707 2004. Code intercomparison builds confidence in numerical simulation models for
708 geologic disposal of CO_2. Energy, 29(9-10), 1431-1444.

709 Puckette, J., Al-Shaieb, Z., 2003. Naturally underpressured reservoirs: applying the
710 compartment concept to the safe disposal of liquid waste. In: search and discovery
711 article 40071, online adaptation of presentation at American Association of
712 Petroleum Geologists, southwest section meeting, Fort Worth, TX, USA, March,
713 2003 (www.southwestsection.org).

714 Rutqvist, J., Tsang, C.F., 2002. A study of caprock hydromechanical changes associated
715 with CO_2-injection into a brine formation. Environ. Geol. 42, 296-305.

716 Rutqvist, J., Birkholzer, J.T., Cappa, F., Tsang, C.F., 2007. Estimating maximum
717 sustainable injection pressure during geological sequestration of CO_2 using coupled
718 fluid flow and geomechanical fault-slip analysis. Energy Convers. Manage. 48,
719 1798-1807.

720 Shafeen, A., Croiset, E., Douglas, P.L., Chatzis, I., 2004. CO_2 sequestration in Ontario,
721 Canada, Part I: storage evaluation of potential reservoirs. Energy Convers. Manage.
722 45, 2645–2659.

723 Stevens, S.H., Pearce, J.M., Rigg, A.A.J., 2001. Natural analog for geologic storage of
724 CO_2: An integrated global research program, in the Proceedings of First National
725 Conference of Carbon Sequestration, National Energy Technology Laboratory,
726 Washington D.C., USA, May 15-17, 2001.

727 USDOE (U.S. Department of Energy), 2007. Methodology for development of carbon
728 sequestration capacity estimates, Appendix A in Carbon Sequestration Atlas of the
729 United States and Canada, National Energy Technology Laboratory, Pittsburgh,
730 PA, USA.

731 USEPA (U.S. Environmental Protection Agency), 1994. Determination of Maximum
732 Injection Pressure for Class I Wells, United States Environmental Protection
733 Agency Region 5—Underground Injection Control Section Regional Guidance #7.
734 EPA, Washington DC, USA.

735 Van der Meer, L.G.H., 1992. Investigations regarding the storage of carbon dioxide in
736 aquifers in the Netherlands. Energy Convers. Manage. 33 (5–8), 611–618.

737 Van der Meer, L.G.H., 1995. The CO_2 storage efficiency of aquifers. Energy Convers.
738 Manage. 36(6–9), 513–518.

739 Van Genuchten, M.T., 1980. A closed form equation for predicting the hydraulic
740 conductivity of unsaturated soils. Soil Sci. Soc. Am. J. 44, 892–898.

Figure 1. Schematic showing open systems versus closed or semi-closed systems (not to scale)

Figure 2. Spatial distributions, simulated at 30 years of CO_2 injection, of (a) CO_2 saturation and (b) pressure buildup for the base case with the closed domain of a 20 km radial extent, and (c) CO_2 saturation and (d) pressure buildup for the case of a closed domain of 100 km radial extent. Figures 2a and 2c show close-ups of the CO_2 plume region with two-phase flow of CO_2 and brine

Figure 3. Pressure-buildup profiles along the aquifer top at different injection times. Filled squares indicate the CO_2 plume extent to show the radial extent of the evolving two-phase flow region

Figure 4. Horizontal profiles of pressure buildup at different times of CO_2 injection for formation permeability of (a) 10^{-12} and (b) 5×10^{-14} m^2, and pore compressibility of (c) 4.5×10^{-9} and (d) 4.5×10^{-11} Pa^{-1}. All other parameters are kept the same as the base case. See comparison with Figure 3

Figure 5. Horizontal profiles of pressure buildup along the aquifer top at different times of CO_2 injection for seal permeability of (a) 10^{-20}, (b) 10^{-19}, (c) 10^{-18}, and (d) 10^{-17} m^2. See comparison with Figure 3

Figure 6. Comparison of the transient profiles of domain-averaged pressure buildup obtained through numerical simulations and through the quick-assessment method for (a) a closed system with varying radial extents R, (b) a closed system with radial extent $R = 20$ km and varying formation permeability, (c) a closed system with radial extent $R = 20$ km and varying pore compressibility, and (d) a semi-closed system with radial extent $R = 20$ km and seals of varying permeability (ks)

765 Table 1. Hydrogeologic properties for the storage formation and CO_2 injection rate used
766 in the base-case simulations

767 Table 2. Numerical simulation runs for different radial extents of storage formation, and
768 different values of permeability and pore compressibility of the storage
769 formation, as well as permeability of the seals

770 Table 3. Comparison of the actual storage efficiency factors for CO_2 storage in closed
771 systems, obtained through numerical simulation results and the quick-
772 assessment method in Equation (5), at 30 years of injection

773 Table 4. Comparison between simulated and estimated volumetric fractions of
774 displaced brine stored in the storage formation, in the seals, and in the
775 overlying and underlying formations, relative to the total pore volume
776 occupied by CO_2 at the end of the 30-year injection period, for different seal
777 permeability values

778

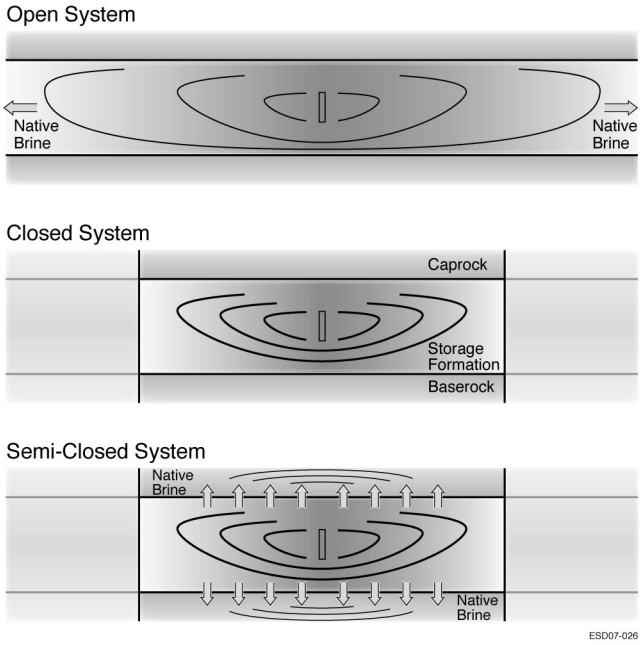

779

780 Figure 1.

781

782

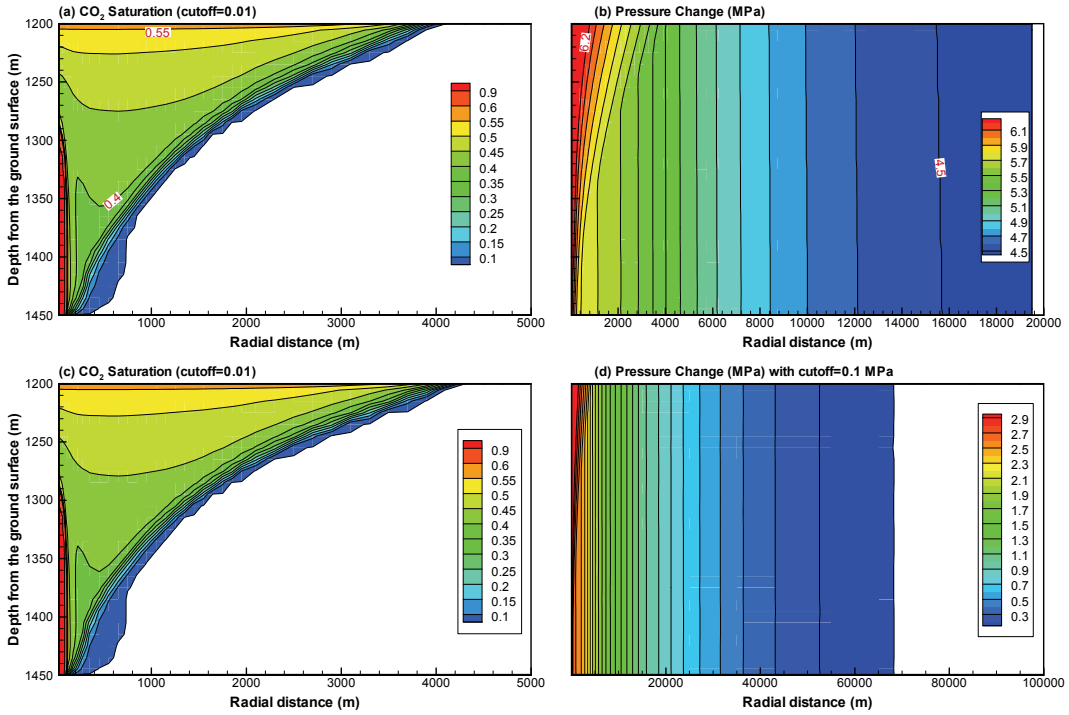

783

784 Figure 2.

785

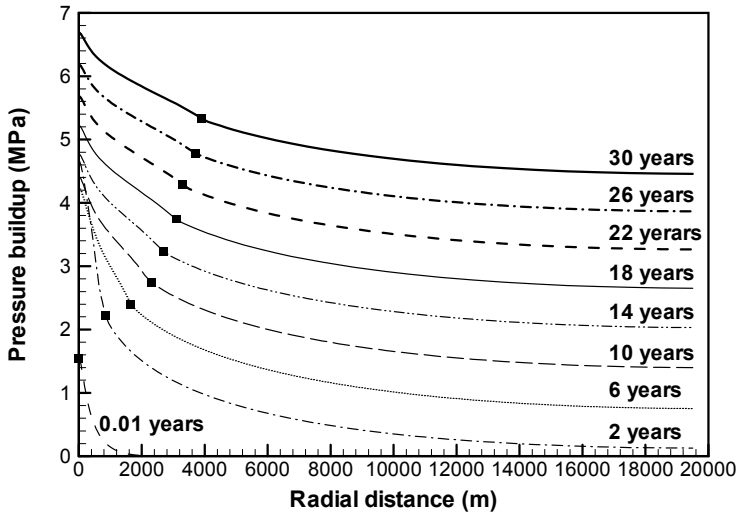

786

787 Figure 3.

788

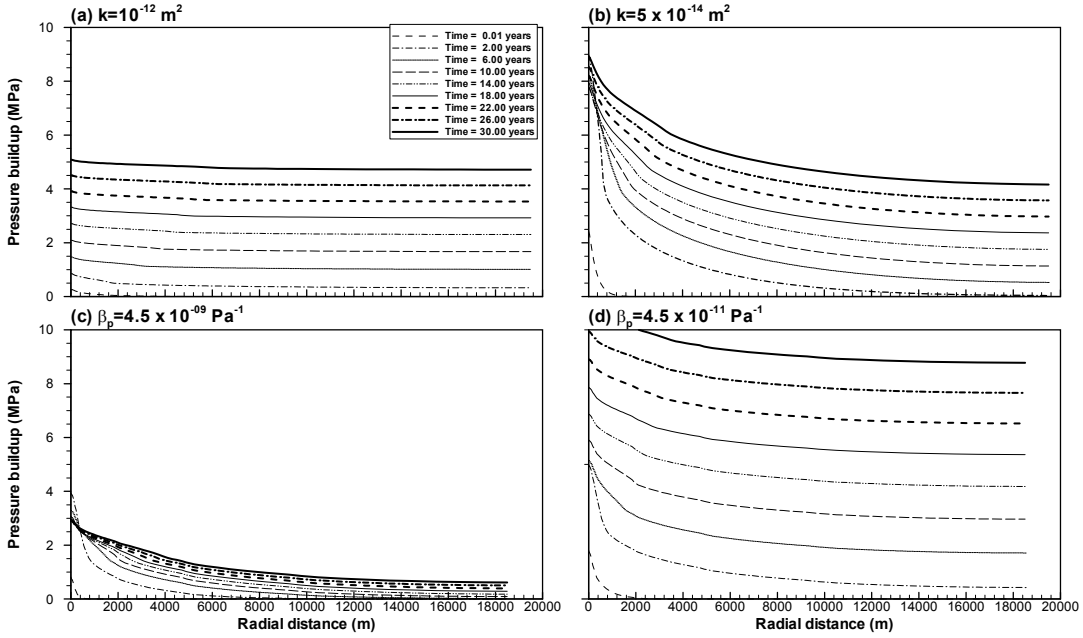

789

790

791 Figure 4.

792

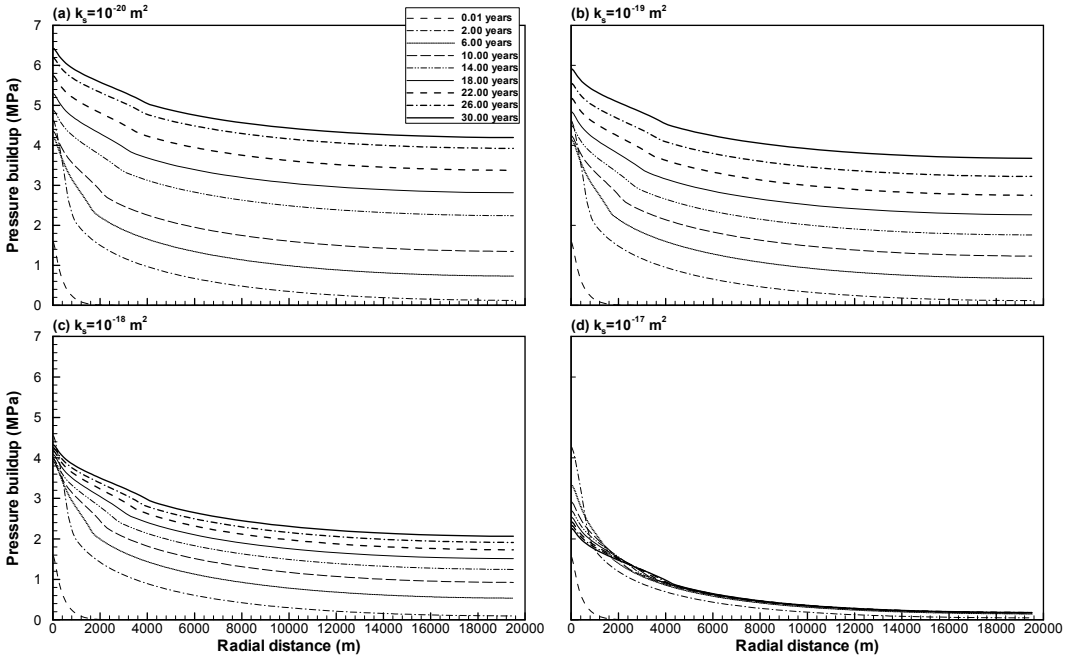

793

794 Figure 5.

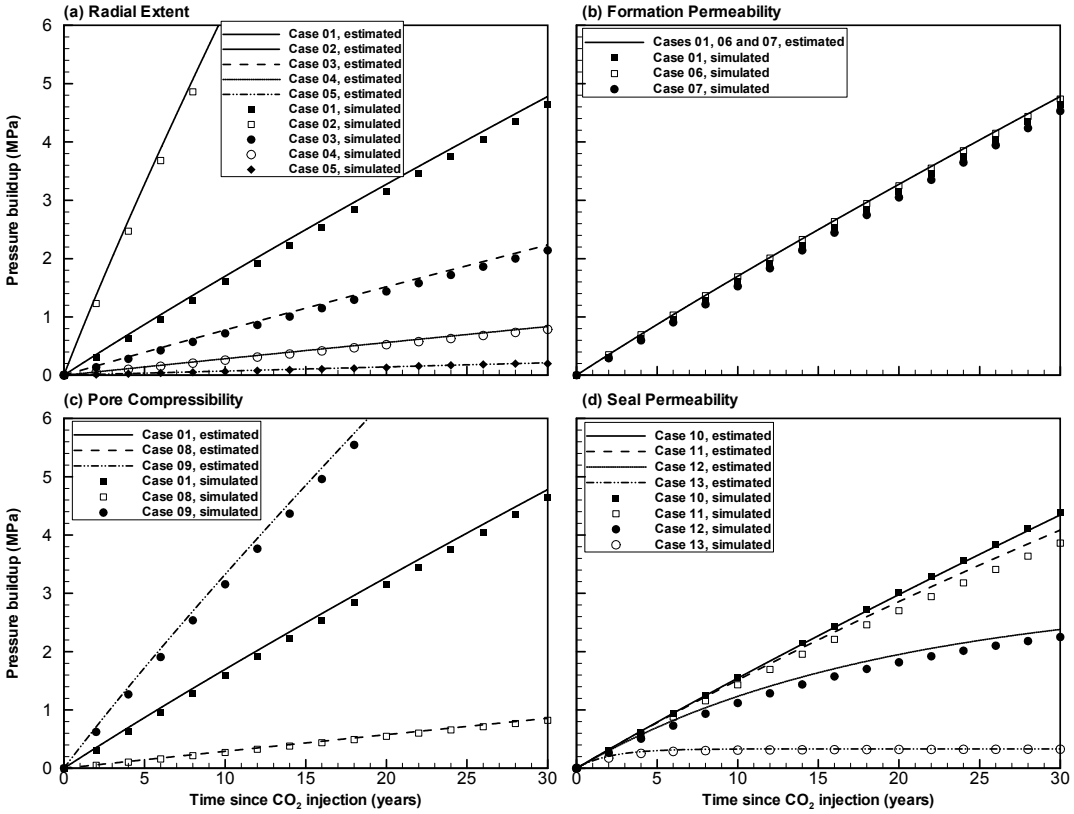

795

796 Figure 6.

797 Table 1.

Properties	**Values**
Horizontal permeability (m^2)	10^{-13}
Vertical permeability (m^2)	10^{-13}
Pore Compressibility (Pa^{-1})	4.5×10^{-10}
Porosity	0.12
van Genuchten (1980) *m*	0.46
van Genuchten α (Pa^{-1})	5.1×10^{-5}
Residual CO_2 saturation	0.05
Residual water saturation	0.30
CO_2 injection rate (kg/s)	120

798

799 Table 2.

	Case No	Radial Extent (km)	Formation Permeability (m^2)	Formation Compressibility (Pa^{-1})	Seal Permeability (m^2)
Base Case	Case 1	20	1.0×10^{-13}	4.5×10^{-10}	0
Storage Formation Volume	Case 2	10	1.0×10^{-13}	4.5×10^{-10}	0
	Case 3	30	1.0×10^{-13}	4.5×10^{-10}	0
	Case 4	50	1.0×10^{-13}	4.5×10^{-10}	0
	Case 5	100	1.0×10^{-13}	4.5×10^{-10}	0
Formation Permeability	Case 6	20	1.0×10^{-12}	4.5×10^{-10}	0
	Case 7	20	5.0×10^{-14}	4.5×10^{-10}	0
Formation Compressibility	Case 8	20	1.0×10^{-13}	4.5×10^{-09}	0
	Case 9	20	1.0×10^{-13}	4.5×10^{-11}	0
Seal Permeability	Case 10	20	1.0×10^{-13}	4.5×10^{-10}	1.0×10^{-20}
	Case 11	20	1.0×10^{-13}	4.5×10^{-10}	1.0×10^{-19}
	Case 12	20	1.0×10^{-13}	4.5×10^{-10}	1.0×10^{-18}
	Case 13	20	1.0×10^{-13}	4.5×10^{-10}	1.0×10^{-17}

800

801 Table 3.

		Simulation-Based Results			Quick-Assessment Estimates
Domain Radius (km)	Initial Pore Volume (10^9 m^3)	Total Stored CO_2 Volume[a] (10^9 m^3)	Average Pressure Buildup Δp (MPa)	Actual Storage Efficiency Factor	Actual Storage Efficiency Factor
100	942.5	0.139	0.2	0.00015	0.00017
50	235.6	0.138	0.79	0.00059	0.00066
30	84.8	0.136	2.14	0.0016	0.0018
20	37.7	0.131	4.64	0.0035	0.0039
10	9.4	0.117	16.60[b]	0.0124	0.014[b]

802 [a] Injected mass is identical for all domains. Stored volumes differ slightly because of different
803 pressure/density conditions.

804 [b] Average pressure buildup is higher than sustainable threshold. The calculated actual storage efficiency is
805 therefore not feasible.

806

807

808 Table 4.

Seals Permeability	Simulation Results			Estimation by Equation (3)		
	Storage Formation	Seals	Other Formations	Storage Formation	Seals	Other Formations
10^{-17} m^2	0.071	0.011	0.918	0.069	0.007	0.925
10^{-18} m^2	0.470	0.104	0.426	0.500	0.050	0.450
10^{-19} m^2	0.824	0.150	0.026	0.850	0.085	0.065
10^{-20} m^2	0.931	0.059	0.010	0.903	0.090	0.007

809